Int. J. Heat Mass Transfer. Vol. 10, pp. 1801–1813. Pergamon Press Ltd. 1967. Printed in Great Britain

FORCED CONVECTIVE HEAT TRANSFER IN UNIFORMLY HEATED HORIZONTAL TUBES

(2ND REPORT, THEORETICAL STUDY)

YASUO MORI† and KOZO FUTAGAMI‡

Department of Mechanical Engineering, Tokyo Institute of Technology, Meguro-ku, Tokyo

(*Received* 2 *April* 1967)

Abstract—Effects of buoyancy force on forced laminar convective heat transfer in a uniformly heated horizontal tube may not be neglected at large *Re Ra*. This 2nd report deals with a theoretical investigation of this problem on a fully developed laminar flow and compares the results with experimental results reported in the 1st report.

In order to back up assumptions made in the following analysis, patterns of secondary flow due to buoyancy are observed in flow visualization experiments. An approximate solution for very large *Re Ra* is obtained. Nusselt numbers are shown as a function of *Re Ra* and *Pr* and are shown to be in fairly good agreement with experimental results on air. Resistance coefficients are also obtained as a function of *Re Ra* and *Pr*.

NOMENCLATURE

a, inside radius of a tube;
C, dimensionless pressure gradient along the tube axis;
C_p, specific heat of fluid at constant pressure;
g, gravitational acceleration;
P, pressure;
q, heat flux at the wall;
r, co-ordinate in radial direction;
t, fluid temperature;
t_w, wall temperature;
t_m, mixed mean temperature;
U, V, W, x, y and z component of velocity in a core flow;
u, v, w, r, ϕ and z component of velocity in a boundary layer;
W_m, mean velocity in the axial direction;
x, horizontal co-ordinate in a cross section perpendicular to the tube axis;
y, vertical co-ordinate in a cross section perpendicular to the tube axis;
z, co-ordinate in the axial direction;
Nu, Nusselt number, $Nu = 2a\alpha/\lambda$;
Pr, Prandtl number, $Pr = \nu/\varkappa$;
Ra, Rayleigh number, $Ra = g\beta a^4\tau/\varkappa\nu = Ra^*/16$, Ra^* is conventional Rayleigh number;
Re, Reynolds number, $Re = 2aW_m/\nu$.

Greek symbols

α, heat-transfer coefficient in the fully developed region;
β, coefficient of volumetric expansion;
γ, specific weight;
δ, δ_T, thickness of the velocity and the thermal boundary layer;
ζ, ratio of thicknesses of boundary layer, $\zeta = \delta/\delta_T$;

† Professor.

‡ Assistant professor, Department of Mechanical Engineering, Ehime University, Matsuyama, Ehime.

Θ, dimensionless temperature in a core flow, $\Theta = g\beta a^3(t_w - t)/\nu^2$;
θ, dimensionless temperature in the boundary layer, $\theta = g\beta a^3(t_w - t)/\nu^2$;
$\varkappa$, thermal diffusivity of fluid;
Λ, resistance coefficient;
λ, thermal conductivity of fluid;
ν, kinematic viscosity;
ξ, co-ordinate, $\xi = 1 - r/a$;
ρ, density of fluid;
τ, temperature gradient along the tube axis, $\tau = \mathrm{d}t_w/\mathrm{d}z$;
ϕ, circumferential co-ordinate from the bottom of a cross section perpendicular to the tube axis.

Subscripts

c, value at the tube axis;
0, value at the tube wall;
m, mean value in the circumferential direction;
δ, value at the outer side of the velocity boundary layer;
δ_T, value at the outer side of the thermal boundary layer.

1. INTRODUCTION

CONCERNING heat transfer to a fully developed laminar flow in a uniformly heated straight circular tube, it is well-known that when the flow has the Poiseuille velocity distribution, the Nusselt number is 48/11. However, when the products of Reynolds number (Re) and Rayleigh number (Ra) are large, effects of free convection are unable to be neglected. A theoretical analysis of this problem was done by Morton [1] by means of a perturbation method, and the result was shown by the form of the positive power series for $ReRa$, but the applicable region is limited to $ReRa < 3000$. Recently, the experimental work for local Nusselt numbers has been carried out by McComas and Eckert [2].

It is worthwhile emphasizing that in laminar convective heat transfer in a uniformly heated tube, the Nusselt number is 48/11 when the temperature difference between fluid and tube wall is negligibly small. However, in a practical case, when the temperature difference would be very large, velocity profiles are very different from the Poiseuille profile and the flow should not be analysed by a perturbation method. We [3] have reported on the results of heat-transfer experiments in air at large $ReRa$ and have shown that the velocity and temperature profiles are much different from those obtained from an analysis neglecting secondary flows or calculated by a perturbation method. In the present report, a theoretical analysis for large $ReRa$ is treated under the assumption based on the 1st report and observations of flows.

Flows in a curved tube, including a strong secondary flow due to centrifugal force, have been investigated in several papers [4, 5, 6, 7]. Analytical methods in those papers are useful for solving the problems such as a secondary flow due to other body forces, in our case buoyancy, because the problem for large $ReRa$ in a horizontal straight tube is considered to correspond to that for large Dean number in a curved tube. However, in an analysis of flow and temperature fields including a secondary flow due to buoyancy, there is an essentially different point which is required to simultaneously solve momentum and energy equations.

2. OBSERVATION OF FLOW PATTERNS WITH SECONDARY FLOW

As the product of $ReRa$ reaches about 10^5, the velocity and the temperature distributions in a cross section perpendicular to a tube axis show a remarkable difference from those of Poiseuille flow, as shown in the 1st report. The region of sharp change of velocity and temperature profiles is affected by a pair of vortices symmetrical against a vertical plane containing the tube axis. In order to confirm patterns of this secondary flow at large $ReRa$, visualization experiments are done.

The apparatus for visualization is almost

similar to that in the 1st report, but the settling chamber has an electrical heater in it and the test section consists of transparent double tubes. Air heated in the settling chamber is sent to the brass circular tube having a 30-mm I.D. and 3 m in length. Downstream from the entrance region, the heat-transfer section is installed. This section of transparent double tube is 30-mm in inner diameter and 3·7 m in length, and cooling air flows in an upstream direction to keep the inner wall temperature gradient in the axial direction constant. Smoke of NH_4Cl is introduced into the air flow in the inner tube at the inlet of the heat-transfer section and the pattern of smoke is photographed. The section for observation is 200-mm long and 500-mm upstream from the tube end, and only this part is illuminated. A few examples of these photographs are shown in Fig. 1. As shown in Fig. 1, the secondary flow forms a pair of vortices, which are symmetrical to the vertical plane and the centers of vortices move closer to the tube wall as $ReRa$ increases. Therefore, at large $ReRa$, it is expected that in heating the fluid, the layer where the flow goes up along the wall tends to become thinner as $ReRa$ increases, and the core flow, with a vertically descending component between both vortices, occupies most of the cross section.

Based on the experiments mentioned above and the results in the 1st report, a flow in a horizontal tube with a secondary flow caused by buoyancy at large $ReRa$ is analyzed in the following part. The flow in the tube may be divided into a flow in a thin layer along the tube wall and a flow in a core region. In the thin layer, velocity and temperature fields are affected by viscosity and thermal conductivity, and boundary-layer approximation may be applied in an analysis. On the other hand, in the core region, velocity and temperature fields are affected mainly by the secondary flow and the effects of viscosity and thermal conductivity may be disregarded.

When the temperature of the tube is higher than that of the fluid, the fluid in the core region goes down due to gravitational force, stagnates at the bottom, goes upwards in the boundary layer along the wall and stagnates again at the top, changing its flow direction. In cooling the fluid, the motion of fluid is quite opposite.

3. ANALYSIS FOR VELOCITY AND TEMPERATURE DISTRIBUTIONS

3.1. *Velocity and temperature distributions in core region*

In a core region, it is assumed that a secondary flow is vertical and uniform; therefore, it is convenient to use the Cartesian co-ordinates as shown in Fig. 2. The following dimensionless quantities are used in the analysis:

$$\left.\begin{aligned} &U^+ = Ua/\nu, \qquad V^+ = Va/\nu, \\ &W^+ = Wa/\nu, \qquad P^+ = a^2P/\rho\nu^2, \\ &\tau^+ = g\beta a^4\tau/\nu^2, \qquad \Theta = g\beta a^3(t_w - t)/\nu^2, \\ &x^+ = x/a, \qquad y^+ = y/a, \qquad z^+ = z/a. \end{aligned}\right\} \quad (1)$$

As a fully developed flow is investigated, $\partial W^+/\partial z^+ = 0$, and by the above assumption for a secondary flow, $V^+ =$ constant and $V^+ < 0$ in heating the fluid, and $V^+ > 0$ in cooling.

When the viscous term and the thermal conductive term are disregarded under the assumption stated above, the equations of motion and energy in the core region become as follows:

$$\frac{\partial P^+}{\partial x^+} = 0 \quad (2)$$

$$\frac{\partial P^+}{\partial y^+} = -\Theta \quad (3)$$

$$V^+\frac{\partial W^+}{\partial y^+} = C \quad (4)$$

where $C = -\partial P^+/\partial z^+$ is a constant in a fully developed flow.

$$-V^+\frac{\partial \Theta}{\partial y^+} + W^+\tau^+ = 0. \quad (5)$$

Integration of the above equation leads to the following relations:

$$W^+ = W_c^+ + (C/V^+)\,y^+ \quad (6)$$

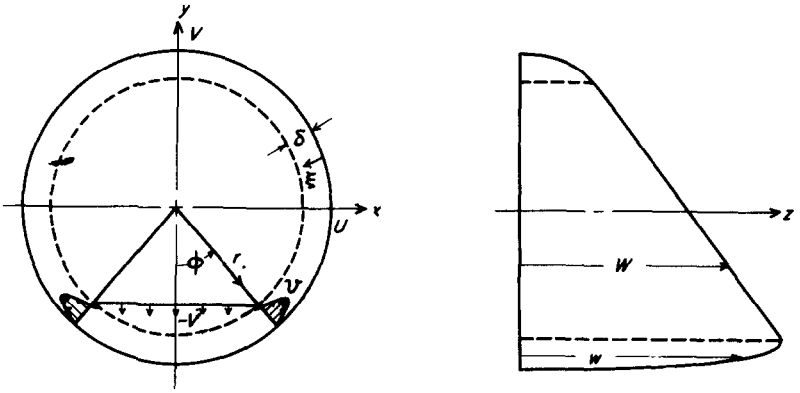

FIG. 2. Co-ordinates.

$$\Theta = \Theta_c + (W_c^+\tau^+/V^+)\,y^+ + (C\tau^+/2V^{+2})\,y^{+2} \tag{7}$$

$$P^+ = P_c^+ - \Theta_c y^+ - (W^+\tau^+/2V^+)\,y^{+2} - (C\tau^+/6V^{+2})\,y^{+3} \tag{8}$$

where W_c^+, Θ_c and P_c^+ are the axial velocity component, the temperature and the pressure at the tube axis, respectively.

From equations (6) and (7), it is clear that the positions of $W_{\max}^+$ and $(\Theta/\Theta_c)_{\max}$ locate downwards from the center in heating the fluid and upwards in cooling. Equations (6–8) are expressed by cylindrical co-ordinates (r, ϕ, z) as follows:

$$W^+ = W_c^+ - \frac{C}{V^+}(1-\xi)\cos\phi \tag{9}$$

$$\Theta = \Theta_c - \frac{W_c^+\tau^+}{V^+}(1-\xi)\cos\phi + \frac{C\tau^+}{2V^{+2}}(1-\xi)^2\cos^2\phi \tag{10}$$

$$P^+ = P_c^+ + (1-\xi)\cos\phi\left\{\Theta_c - \frac{W_c^+\tau^+}{2V^+}(1-\xi)\times\cos\phi + \frac{C\tau^+}{6V^{+2}}(1-\xi)^2\cos^2\phi\right\} \tag{11}$$

hence $\xi = 1 - r/a$.

3.2. *Velocity and temperature distributions in the boundary layer*

It is not easy to obtain an exact solution of the simultaneous equations of momentum and energy for boundary-layer flows. Therefore, we shall try to solve the integral equations of momentum and energy. Let us describe velocities and temperature in a boundary layer by small letters, and use such dimensionless quantities as given in equation (1). The profile of the axial velocity is expressed as follows by a quadratic equation satisfying the boundary conditions, $w_{\xi=0}^+ = 0$, $(\partial w^+/\partial\xi)_{\xi=\delta} = 0$ and $w_{\xi=\delta}^+ = W_\delta^+$ where W_δ^+ is the value of W^+ at $\xi = \delta$ in the core region:

$$w^+ = W_\delta^+\left(2\frac{\xi}{\delta} - \frac{\xi^2}{\delta^2}\right) \tag{12}$$

The circumferential velocity component v^+ in the boundary layer is expressed by a cubic equation satisfying the boundary conditions: $v_{\xi=0}^+ = 0$, $v_{\xi=\delta}^+ = V^+\sin\phi$ and $(\partial v^+/\partial\xi)_{\xi=\delta} = 0$ and the continuity condition expressed by the following equation:

$$\int_0^\delta v^+\,\mathrm{d}\xi = -V^+(1-\delta)\sin\phi \tag{13}$$

and v^+ is

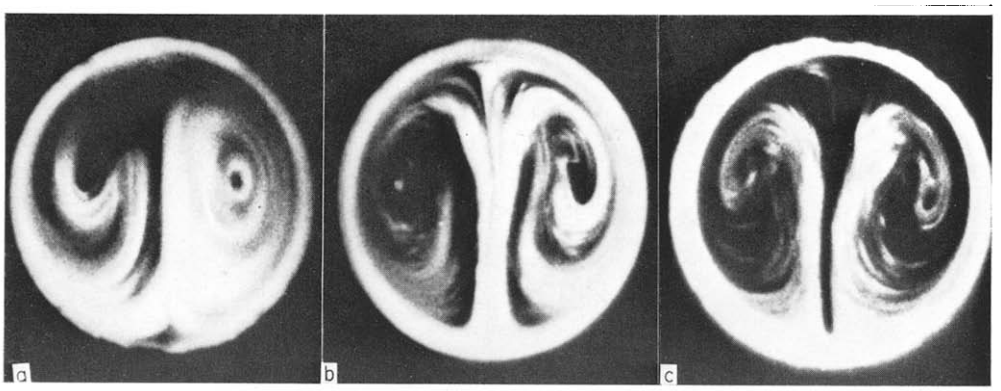

FIG. 1. Secondary flow pattern.
(a) $Re\ Ra = 2\times10^4$ (b) $Re\ Ra = 9\times10^4$ (c) $Re\ Ra = 1{\cdot}6\times10^5$

$$v^+ = -\frac{12V^+}{\delta}\sin\phi \cdot f_1(\eta) \qquad (14)$$

where

$$f_1(\eta) = \eta\left\{(1-\eta)^2 - \frac{\delta}{12}(6 - 9\eta + 4\eta^2)\right\}$$

and

$$\eta = \frac{\xi}{\delta}.$$

Disregarding the smaller terms in equation (14) we get

$$v^+ = -\frac{12V^+}{\delta}\sin\phi \cdot f_2(\eta) \qquad (15)$$

where

$$f_2(\eta) = \eta\left\{(1-\eta)^2 - \frac{\delta}{12}\right\}.$$

The difference between $f_1(\eta)$ and $f_2(\eta)$ in the case of $\delta = 0{\cdot}1$ is very small, as shown in Fig. 3.

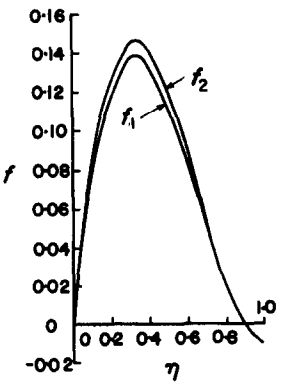

FIG. 3. Comparison of f_1 and f_2.

Defining δ_T as the thickness of a thermal boundary layer, the temperature distribution in the thermal boundary layer is approximated by a quadratic equation satisfying the boundary conditions as follows: $\theta_{\xi=0} = 0$, $\theta_{\xi=\delta_T} = \Theta_{\delta_T}$ (hence Θ_{δ_T} is a value at $\xi = \delta_T$ in core flow) and $(\partial\theta/\partial\xi)_{\xi=\delta_T} = 0$.

$$\theta = \Theta_{\delta_T}\left(2\frac{\xi}{\delta_T} - \frac{\xi^2}{\delta_T^2}\right). \qquad (16)$$

3.3. *Determination of* W_c^+, Θ_c *and* C

In considering the balance of axial forces of a fluid element enclosed by a tube wall and two cross sections with an interval dz, we obtain

$$dz^+\int_0^{2\pi}\left(\frac{\partial w^+}{\delta\xi}\right)_0 d\phi = \int_0^{2\pi}\int_0^1\left\{P^+ - \left(P^+ + \frac{\partial P^+}{\partial z^+}dz^+\right)\right\}(1-\xi)\,d\xi\,d\phi. \qquad (17)$$

The left-hand side is a viscous force at the wall and is expressed by equations (9) and (12) as follows:

$$\left(\frac{\partial w^+}{\delta\xi}\right)_0 = \frac{2}{\delta}\left\{W_c^+ - \frac{C}{V^+}(1-\delta)\cos\phi\right\} \qquad (18)$$

δ is a function of ϕ, but it is considered from the experimental results and the analysis [7] for a flow in a curved pipe that variation of δ in ϕ direction is small, therefore when δ is replaced by its mean value δ_m equation (18) becomes,

$$\left(\frac{\partial w^+}{\delta\xi}\right)_0 = \frac{2}{\delta_m}\left\{W_c^+ - \frac{C}{V^+}(1-\delta_m)\cos\phi\right\}. \qquad (19)$$

By integrating equation (17) in substitution of equation (19), we get

$$C = 4W_c^+/\delta_m. \qquad (20)$$

The dimensionless mean velocity W_m^+ is shown by Reynolds number from equation (1) as

$$W_m^+ = Re/2. \qquad (21)$$

On the other hand, W_m^+ is expressed as

$$W_m^+ = \frac{1}{\pi}\int_0^{2\pi}\left\{\int_0^{\delta_m} w^+(1-\xi)\,d\xi + \int_{\delta_m}^1 W^+(1-\xi)\,d\xi\right\}d\phi.$$

Integration of this equation by use of equations (9) and (12), leads to

$$W_m^+ = W_c^+(1 - \tfrac{2}{3}\delta_m + \tfrac{1}{6}\delta_m^2). \quad (22)$$

From equations (21) and (22), W_c^+ is given as follows:

$$W_c^+ = \frac{Re}{2}\frac{1}{(1 - \frac{2}{3}\delta_m + \frac{1}{6}\delta_m^2)}. \quad (23)$$

From equation (20), we obtain

$$C = \frac{2Re}{\delta_m}\frac{1}{(1 - \frac{2}{3}\delta_m + \frac{1}{6}\delta_m^2)}. \quad (24)$$

When δ_m is sufficiently small compared with unity, W_c^+ and C are shown as follows:

$$W_c^+ = Re/2 \quad (25)$$

$$C = 2Re/\delta_m. \quad (26)$$

Considering heat balance of a fluid element, we have

$$\pi W_m^+ Pr\,\tau^+ = \int_0^{2\pi}\left(\frac{\partial\theta}{\partial\xi}\right)_0 d\phi. \quad (27)$$

Substitution of equations (10) and (16) in the right side of equation (27) leads to

$$W_m^+ Pr\,\tau^+ = \frac{4\zeta_m}{\delta_m}\left(\Theta_c + \frac{C\tau^+}{4V^{+2}}\right) \quad (28)$$

where $\zeta_m = \delta_m/\delta_{Tm}$ and $Pr\ \tau^+$ is given by Rayleigh number as $Pr\,\tau^+ = Ra$. By substituting equations (21) and (24) in equation (28), Θ_c is shown as follows:

$$\Theta_c = \frac{ReRa}{8}\delta_m\left\{\frac{1}{\zeta_m} - \frac{4}{V^{+2}\delta_m^2}\frac{1}{Pr} \times \frac{1}{(1 - \frac{2}{3}\delta_m + \frac{1}{6}\delta_m^2)}\right\}. \quad (29)$$

When $\delta_m \ll 1$, equation (29) can be written as,

$$\Theta_c = \frac{ReRa}{8}\delta_m\left\{\frac{1}{\zeta_m} - \frac{4}{V^{+2}\delta_m^2}\frac{1}{Pr}\right\}. \quad (30)$$

From the above relations, velocity and temperature distributions are shown as functions of ξ and ϕ with unknown quantities V^+, δ_m and ζ_m.

3.4. *Boundary-layer equations*

The thickness of a boundary layer is assumed to be sufficiently small compared with the radius of the tube at large $ReRa$. Before carrying out an analysis, we have to investigate the order of magnitude of the terms in the fundamental equations.

The following dimensionless quantities are used in the order estimation.

$$v' = v/v_{max}, \quad u' = u/v_{max}, \quad w' = w/W_m,$$
$$P' = P/\rho v_{max}^2, \quad \theta' = (t_w - t)/(t_w - t_c),$$
$$\xi = 1 - r/a, \quad z^+ = z/a$$

Hence v_{max} is the maximum value of circumferential velocity component, W_m the mean value of axial velocity component and t_c the temperature at the center of the tube.

Neglecting smaller terms than $0(\delta)$ in the equations of motion and energy and considering $\xi = 0(\delta)$, $v' = 0(1)$, $u' = 0(\delta)$ and $\theta' = 0(1)$, we obtain the fundamental equations for the boundary layer. These equations are represented by use of the same dimensionless quantities as equation (1) as follows:

continuity equation:

$$\frac{\partial u^+}{\partial\xi} = \frac{\partial v^+}{\partial\phi}, \quad (31)$$

equation of motion:

$$-v^{+2} = \frac{\partial P^+}{\partial\xi} + \theta\cos\phi \quad (32)$$

$$-u^+\frac{\partial v^+}{\partial\xi} + v^+\frac{\partial v^+}{\partial\phi} = -\frac{\partial P^+}{\partial\phi} + \frac{\partial^2 v^+}{\partial\xi^2} - \theta\sin\phi \quad (33)$$

$$-u^+\frac{\partial w^+}{\partial\xi} + v^+\frac{\partial w^+}{\partial\phi} = C + \frac{\partial^2 w^+}{\partial\xi^2} \quad (34)$$

energy equation:

$$u^+\frac{\partial\theta}{\partial\xi} - v^+\frac{\partial\theta}{\partial\phi} + w^+\tau^+ = -\frac{1}{Pr}\frac{\partial^2\theta}{\partial\xi^2}, \quad (35)$$

where the dissipation and pressure terms in the energy equation are neglected because Mach number is small.

3.5. *Integral equation of momentum*

3.5.1. *Equation in axial direction.* Integrating equation (34) from zero to δ with respect to ξ by the aid of equation (31), the integral equation of momentum is obtained as

$$-W_\delta^+\frac{\partial}{\partial\phi}\int_0^\delta v^+\,\mathrm{d}\xi + \frac{\partial}{\partial\phi}\int_0^\delta v^+w^+\,\mathrm{d}\xi - C.\delta = -\left(\frac{\partial w^+}{\partial\xi}\right)_0. \quad (36)$$

The integrals in this equation are computable by means of equations (9), (12) and (15). Replacing δ with its mean value δ_m, the result is

$$-\tfrac{3}{5}C(1-\tfrac{1}{3}\cos^2\phi) + \tfrac{2}{5}W_c^+V^+\cos\phi = -\frac{2}{\delta_m}\left(W_c^+ - \frac{C}{V^+}\cos\phi\right) \quad (37)$$

Taking the mean value of equation (37) over ϕ, equation (37) is reduced as follows:

$$C = 4W_c^+/\delta_m.$$

This is the same relation as equation (20) obtained from the balance of axial forces. In other words, the profiles assumed by equations (12) and (15) satisfy the mean value of equation (36) over ϕ, but it does not mean that they satisfy equation (36) at any value of ϕ. The first term of the left side in equation (37) is a function of ϕ, but the variation from the mean value is small compared with the second term as shown in Fig. 4; therefore, the first term can be replaced by the mean value $-C/2$ and the relation between V^+ and δ_m is led from the coefficients of $\cos\phi$ in equation (37)

$$V^+.\delta_m = \pm\sqrt{20} \quad (38)$$

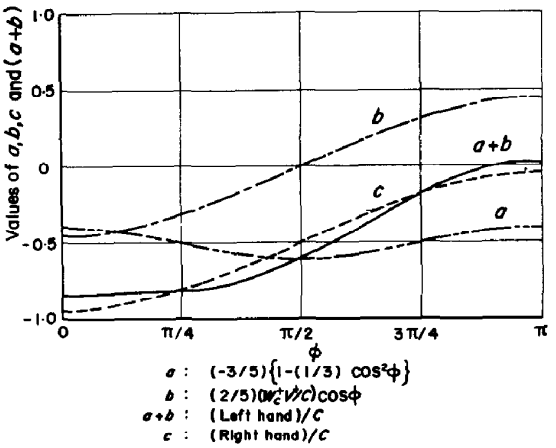

FIG. 4. Variation of each term along ϕ in equation (37).

where we choose the positive sign for cooling the fluid and the negative sign for heating. The comparison of the variations in ϕ for each term of equation (37) is shown in Fig. 4, by use of equation (38).

3.5.2. *Equation in circumferential direction.* As equations (32) and (33) contain the velocity components and the temperature, integral limits must be carefully taken.

(a) $\qquad \delta \leqslant \delta_T (\zeta \leqslant 1).$

The pressure term in equation (33) can be obtained by integrating equation (32) from ξ to δ_T with respect to ξ and shown as

$$\frac{\partial P^+}{\partial\phi} = \frac{\partial}{\partial\phi}\int_\xi^\delta v^{+2}\,\mathrm{d}\xi + \frac{\partial}{\partial\phi}V^{+2}\sin^2\phi\,(\delta_T-\delta) + \frac{\partial}{\partial\phi}\int_\xi^{\delta_T}\theta\cos\phi\,\mathrm{d}\xi + \frac{\partial p^+_{\delta_T}}{\partial\phi}$$

where $P^+_{\delta_T}$ shows the value of equation (11) at $\xi = \delta_T$.

The integral momentum equation of the boundary layer in the circumferential direction is obtained by substitution of the above equation in equation (33) and integrating it from zero to δ_T with respect to ξ.

$$-V^{+}\sin\phi\frac{\partial}{\partial\phi}\int_0^{\delta}v^{+}\,\mathrm{d}\xi-V^{+2}\sin\phi\frac{\partial}{\partial\phi}\times(\delta_T-\delta)\sin\phi+\frac{\partial}{\partial\phi}\int_0^{\delta}v^{+2}\,\mathrm{d}\xi+V^{+2}\frac{\partial}{\partial\phi}(\delta_T-\delta)\sin^2\phi=-\int_0^{\delta_T}\frac{\partial P^{+}}{\partial\phi}\,\mathrm{d}\xi-\left(\frac{\partial v^{+}}{\partial\xi}\right)_0-\int_0^{\delta_T}\theta\sin\phi\,\mathrm{d}\xi. \quad (39)$$

Substituting equations (15) and (16), equation (39) can be integrated. When δ_{T_m} is sufficiently small compared with unity, and small terms in it are neglected, it is reduced as follows:

$$\frac{96}{35}\frac{V^{+2}}{\delta_m}\cos\phi=\frac{1}{3}\frac{\delta_m^2}{\zeta_m}\times ReRa\left\{\frac{1}{8}\left(\frac{1}{\zeta_m}-\frac{4}{V^{+2}\delta_m^2}\frac{1}{Pr}\right)-\frac{\cos\phi}{2V^{+}\delta_m Pr}+\frac{\cos^2\phi}{V^{+2}\delta_m^2 Pr}\right\}+12\frac{V^{+}}{\delta_m^2}. \quad (40)$$

Eliminating V^{+} from equations (38) and (40), the relation between δ_m and ζ_m is obtained.

$$\frac{384}{7}\frac{1}{\delta_m^3}\cos\phi=\frac{1}{3}\frac{\delta_m^2}{\zeta_m Pr}ReRa\left\{\frac{1}{8}\left(\frac{Pr}{\zeta_m}-\frac{1}{5}\right)\mp\frac{\cos\phi}{2\sqrt{20}}+\frac{\cos^2\phi}{20}\right\}\pm\frac{12\sqrt{20}}{\delta_m^3}. \quad (41)$$

Taking the mean value of equation (41) over ϕ, we get

$$\delta_m=(288\sqrt{20})^{\frac{1}{4}}\left(\frac{\zeta_m^2}{ReRa}\right)^{\frac{1}{4}}. \quad (42)$$

The other relation for δ_m and ζ_m is found from the coefficients of $\cos\phi$ of equation (41) as

$$\delta_m=\left(\frac{2304\sqrt{20}}{7}\right)^{\frac{1}{4}}\left(\frac{\zeta_m Pr}{ReRa}\right)^{\frac{1}{4}}. \quad (43)$$

A discussion of equations (42) and (43), will be made later.

(b) $\delta\geqslant\delta_T(\zeta\geqslant 1)$.

In the same way as the case of $\delta\leqslant\delta_T$, integrating equations (32) and (33), we obtain

$$-V^{+}\sin\phi\frac{\partial}{\partial\phi}\int_0^{\delta}v^{+}\,\mathrm{d}\xi+\frac{\partial}{\partial\phi}\int_0^{\delta}v^{+2}\,\mathrm{d}\xi=-\frac{\partial}{\partial\phi}\int_0^{\delta}\int_{\xi}^{\delta}v^{+2}\,\mathrm{d}\xi\,\mathrm{d}\xi-\frac{\partial}{\partial\phi}\int_0^{\delta_T}\int_{\xi}^{\delta_T}\theta\cos\phi\,\mathrm{d}\xi\,\mathrm{d}\xi-\frac{\partial}{\partial\phi}\int_{\delta_T}^{\delta}\int_{\delta_T}^{\delta}\Theta\cos\phi\,\mathrm{d}\xi\,\mathrm{d}\xi-\frac{\partial P_{\delta}^{+}}{\partial\phi}\delta-\left(\frac{\partial v^{+}}{\partial\xi}\right)_0-\int_0^{\delta_T}\theta\sin\phi\,\mathrm{d}\xi-\int_{\delta_T}^{\delta}\Theta\sin\phi\,\mathrm{d}\xi. \quad (44)$$

Equation (44) can be integrated, and as long as δ_m is very small compared with unity, small terms may be neglected, and the result is equal to equation (41), δ_m is also shown by equation (42) or (43).

3.6. *Integral equation of energy*

3.6.1. $\delta\leqslant\delta_T$, $(\zeta\leqslant 1)$. Considering that the velocity profile in the core region can be used for the region of $\delta\leqslant\xi\leqslant\delta_T$, the energy integral equation becomes

$$\Theta_{\delta_T}\frac{\partial}{\partial\phi}\int_0^{\delta}v^{+}\,\mathrm{d}\xi+\Theta_{\delta_T}\frac{\partial}{\partial\phi}V^{+}(\delta_T-\delta)\sin\phi-\frac{\partial}{\partial\phi}\int_0^{\delta}\theta v^{+}\,\mathrm{d}\xi-\frac{\partial}{\partial\phi}V^{+}\sin\phi\int_{\delta}^{\delta_T}\theta\,\mathrm{d}\xi+\tau^{+}\int_0^{\delta}w^{+}\,\mathrm{d}\xi+\tau^{+}\int_{\delta}^{\delta_T}W^{+}\,\mathrm{d}\xi=\frac{1}{Pr}\left(\frac{\partial\theta}{\partial\xi}\right)_0. \quad (45)$$

Disregarding small terms, we obtain from equation (45)

$$(-1 + \tfrac{4}{5}\zeta_m - \tfrac{1}{5}\zeta_m^2)\left(\Theta_c V^+ \cos\phi - W_c^+\tau^+ \cos^2\phi + \frac{C\tau^+}{2V^{+2}}\cos^3\phi\right) + (\tfrac{4}{5}\zeta_m - \tfrac{1}{5}\zeta_m^2) \times \left(W_c^+\tau^+ \sin^2\phi - \frac{C\tau^+}{V^+}\sin^2\phi\cos\phi\right) = \frac{2\zeta_m}{Pr\,\delta_m}\left(\Theta_c - \frac{W_c^+\tau^+}{V^+}\cos\phi + \frac{C\tau^+}{2V^{+2}}\cos^2\phi\right). \quad (46)$$

By taking the mean value of equation (46) over ϕ, it reduces to

$$\frac{W_c^+\tau^+}{2} = \frac{2\zeta_m}{Pr\,\delta_m}\left(\Theta_c + \frac{C\tau^+}{4V^{+2}}\right).$$

This relation satisfies equation (28) obtained from heat balance.

From coefficients of cos ϕ of equation (46), we obtain

$$(1 - \tfrac{4}{5}\zeta_m + \tfrac{1}{5}\zeta_m^2)\Theta_c V^+ = \frac{2\zeta_m}{Pr\,\delta_m}\frac{W_c^+\tau^+}{V^+}. \quad (47)$$

By substituting equations (25), (30) and (38) in equation (47), the following equation is introduced:

$$\zeta_m^3\,Pr - \zeta_m^2(5Pr^2 + 4Pr - 10) + 5\zeta_m\,Pr(4Pr + 1) - 25Pr^2 = 0. \quad (48)$$

The thickness ratio $\zeta_m = \delta_m/\delta_{Tm}$ is given as a function of only Prandtl number and its relation is shown in Fig. 5 and $\zeta_m \leqslant 1$ corresponds to $Pr = 1{\cdot}105$. For a specific Prandtl number, the terms in equation (46) vary with ϕ and it is shown in Fig. 6 for $Pr = 1{\cdot}105$. Computation of equations (42) and (43) by use of equation (48) shows that they are in agreement with at most 5 per cent difference for $Pr = 1{\cdot}105$; therefore, equation (42) will be used to calculate δ_m.

3.6.2. $\delta \geqslant \delta_T$, $(\zeta \geqslant 1)$. Considering that the temperature profile in the core region can be extended to the region of $\delta \geqslant \xi \geqslant \delta_T$, the energy integral equation is written as follows:

$$\Theta_\delta \frac{\partial}{\partial\phi}\int_0^\delta v^+\,d\xi - \frac{\partial}{\partial\phi}\int_0^{\delta_T}\theta v^+\,d\xi - \frac{\partial}{\partial\phi}\int_{\delta_T}^{\delta}\Theta v^+\,d\xi + \tau^+\int_0^\delta w^+\,d\xi = \frac{1}{Pr}\left(\frac{\partial\theta}{\partial\xi}\right)_0. \quad (49)$$

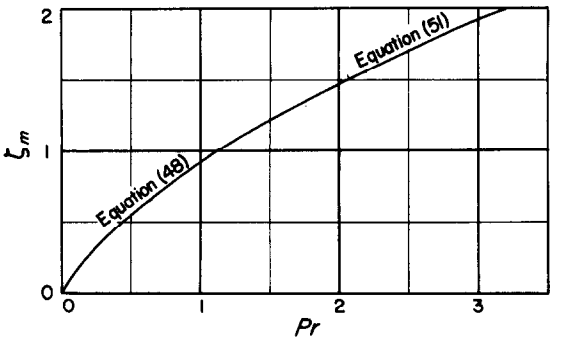

FIG. 5. Relations between ζ_m and Pr.

Calculating the integrals in this equation, we obtain

$$-\frac{1}{\zeta_m^2}\left(1 - \frac{4}{5}\frac{1}{\zeta_m} + \frac{1}{5}\frac{1}{\zeta_m^2}\right)\left(\Theta_c V^+\cos\phi - W_c^+\tau^+\cos^2\phi + \frac{C\tau^+}{2V^{+2}}\cos^3\phi\right) + \left\{1 - \frac{1}{\zeta_m^2}\left(1 - \frac{4}{5}\frac{1}{\zeta_m} + \frac{1}{5}\frac{1}{\zeta_m^2}\right)\right\} \times \left(W_c^+\tau^+\sin^2\phi - \frac{C\tau^+}{V^+}\sin^2\phi\,.\cos\phi\right) = \frac{2\zeta_m}{Pr\,\delta_m}\left(\Theta_c - \frac{W_c^+\tau^+}{V^+}\cos\phi + \frac{C\tau^+}{2V^{+2}}\cos^2\phi\right). \quad (50)$$

The mean value over ϕ of equation (50) satisfies equation (28), and from the coefficients of cos ϕ of equation (50), we obtain

$$10\zeta_m^6 + 5\zeta_m^3\,Pr - (25\,Pr + 4)\zeta_m^2\,Pr + (20\,Pr + 1)\zeta_m\,Pr - 5\,Pr^2 = 0. \quad (51)$$

This relation is shown in Fig. 5 and $\zeta_m \geqslant 1$ corresponds to $Pr \geqslant 1{\cdot}105$.

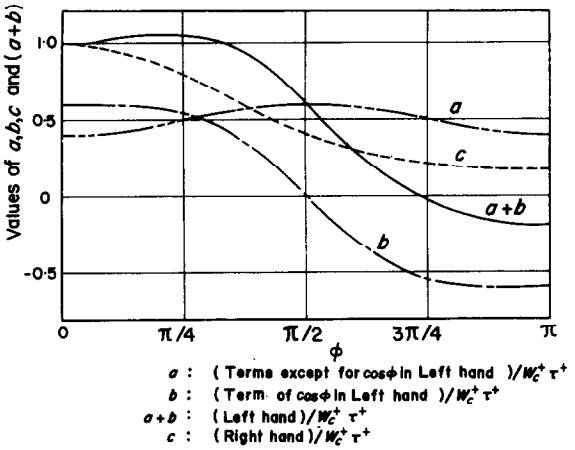

FIG. 6. Variation of each term along ϕ in equation (46).

Thus, V^+, δ_m and ζ_m are determined respectively by equations (38, 42) and (48) or (51).

4. NUSSELT NUMBER

Heat-transfer coefficients α in a fully developed region are defined by

$$\alpha = q/(t_w - t_m) \tag{52}$$

where q is the mean heat flux over ϕ at a section z, given by

$$q = \frac{\lambda}{2\pi}\int_0^{2\pi}\left(\frac{\partial t}{\partial r}\right)_{r=a} \mathrm{d}\phi. \tag{53}$$

Nusselt number is defined by

$$Nu = \frac{2a\alpha}{\lambda} = \frac{4}{\Theta_m}\frac{\zeta_m}{\delta_m}\left(\Theta_c + \frac{C\tau^+}{4V^{+2}}\right) \tag{54}$$

where Θ_m is a dimensionless mixed mean temperature, shown by $\Theta_m = g\beta\alpha^3(t_w - t_m)/\nu^2$ and can be calculated as follows:

for $\delta_m \geqslant \delta_{Tm}$,

$$\Theta_m = \frac{2}{\pi W_m^+}\left\{\int_0^{\pi}\int_1^{\delta_m} \Theta \,.\, W^+(1-\xi)\,\mathrm{d}\xi\,\mathrm{d}\phi + \int_0^{\pi}\int_{\delta_m}^{\delta_{Tm}} \Theta \,.\, w^+(1-\xi)\,\mathrm{d}\xi\,\mathrm{d}\phi\right.$$

$$\left. + \int_0^{\pi}\int_{\delta_{Tm}}^{0} \theta \,.\, w^+(1-\xi)\,\mathrm{d}\xi\,\mathrm{d}\phi\right\}$$

for $\delta_m \leqslant \delta_{Tm}$,

$$\Theta_m = \frac{2}{\pi W_m^+}\left\{\int_0^{\pi}\int_1^{\delta_{Tm}} \Theta \,.\, W^+(1-\xi)\,\mathrm{d}\xi\,\mathrm{d}\phi + \int_0^{\pi}\int_{\delta_{Tm}}^{\delta_m} \theta \,.\, W^+(1-\xi)\,\mathrm{d}\xi\,\mathrm{d}\phi\right.$$

$$\left. + \int_0^{\pi}\int_{\delta_m}^{0} \theta \,.\, w^+(1-\xi)\,\mathrm{d}\xi\,\mathrm{d}\phi\right\}.$$

Assuming δ_m and $\delta_{Tm} \ll 1$ and neglecting smaller terms, the integration of the above equation leads to

$$\Theta_m = \Theta_c + \frac{3}{8}\frac{C\tau^+}{V^{+2}}. \tag{55}$$

Substitution of equation (55) into equation (51) introduces Nusselt number ratio Nu/Nu_0 as

$$\frac{Nu}{Nu_0} = 0{\cdot}2189\frac{(Re\,Ra)^{\frac{1}{4}}}{\left(\frac{1}{\zeta_m} + \frac{1}{10\,Pr}\right)\zeta_m^{\frac{1}{4}}} \tag{56}$$

where Nu_0 is Nusselt number for forced convective heat transfer under the assumption of Poiseuille flow in a uniformly heated tube and $Nu_0 = 48/11$, ζ_m is shown by equation (48) or (51). Equation (56) is applicable in a region when Prandtl number is not far away from unity.

5. RESISTANCE COEFFICIENT

Resistance coefficients Λ for a fully developed forced laminar flow in a horizontal tube are also affected by a secondary flow. The definition of resistance coefficient is expressed by

$$\Lambda = \frac{4C}{W_m^{+2}}.$$

The assumption that $\delta_m \ll 1$ and substitution of

equations (21) and (26) in this equation give Λ and the ratio of resistance coefficients, Λ/Λ_0 is calculated by

$$\frac{\Lambda}{\Lambda_0} = \frac{1}{2\delta_m} = 0{\cdot}1195\frac{(ReRa)^{\frac{1}{4}}}{\zeta_m^{\frac{1}{4}}} \tag{57}$$

where Λ_0 shows the resistance coefficient for Poiseuille flow and $\Lambda_0 = 64/Re$. From equation (57), it is clear that resistance coefficients also increase with increasing $ReRa$. An increase of Prandtl number causes a decrease of resistance coefficient, because the thickness of the velocity boundary layer increases as shown by equation (42).

6. DISCUSSION OF RESULTS

6.1. *Velocity and temperature distributions*

The profiles of velocity and temperature in the core region are given by equations (9) and (10) and expressed as follows:

$$\left.\begin{aligned}\frac{W^+}{W_c^+} &= 1 \pm \frac{2}{\sqrt{5}}\frac{r}{a}\cos\phi \\ \frac{\Theta}{\Theta_c} &= 1 \pm \frac{2\sqrt{5}}{5\dfrac{Pr}{\zeta_m} - 1}\frac{r}{a}\cos\phi \\ &\quad + \frac{2}{5\dfrac{Pr}{\zeta_m} - 1}\left(\frac{r}{a}\right)^2\cos^2\phi\end{aligned}\right\} \tag{58}$$

where the double sign takes positive for heating the fluid and negative for cooling, and the profile in $\phi = 0$ or π shows one in the vertical plane and that in $\phi = \pi/2$ or $3\pi/2$ shows one in the horizontal plane. These equations were obtained on the assumption that $\delta_m \ll 1$ or $\delta_{Tm} \ll 1$ and the condition for $\delta_m \leqslant 0{\cdot}1$ is obtained when $ReRa \geqslant 6{\cdot}67 \times 10^7$ for $Pr = 0{\cdot}72$ from equation (42). These results are asymptotic solutions for large $ReRa$. Comparisons with experimental data [3] with $ReRa$ of about 10^5 for air ($Pr = 0{\cdot}72$) are shown in Fig. 7 for velocity profile and in Fig. 8 for temperature profile.

Equation (58) does not contain $ReRa$ but the experimental results are affected by $ReRa$ and tend to approach to the theoretical profile with increasing $ReRa$. This is due to the fact that experiments are not done at $ReRa$ large enough to neglect δ_m compared with unity. In calculating heat-transfer coefficients, a mixed mean temperature in the core region is an important factor, and in spite of little difference between theoretical and experimental profiles, the mixed mean temperatures in both profiles are nearly equal, therefore it is considered that heat-transfer coefficients calculated from experimental results are in rather good agreement with theoretical prediction.

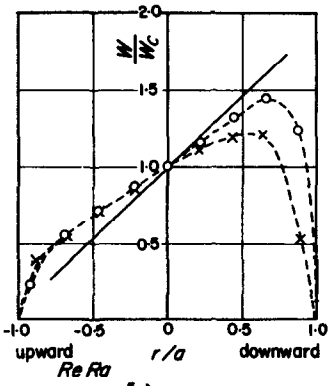

FIG. 7. Velocity distributions at $\phi = 0, \pi$.

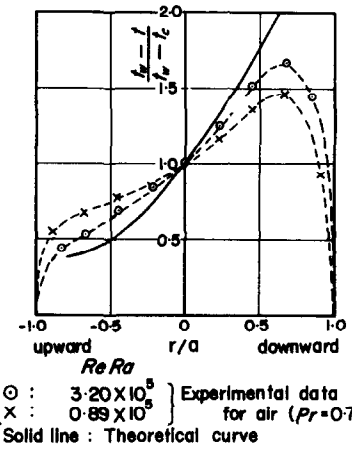

FIG. 8. Temperature distributions at $\phi = 0, \pi$.

6.2. *Nusselt number*

From equation (56), we obtain

$$Nu/Nu_0 = 0{\cdot}1634\,(ReRa)^{\frac{1}{4}} \quad \text{for} \quad Pr = 0{\cdot}72 \tag{59}$$

$$Nu/Nu_0 = 0{\cdot}1929\,(ReRa)^{\frac{1}{4}} \quad \text{for} \quad Pr = 1. \tag{60}$$

With Prandtl number as a parameter, the relations of Nu/Nu_0 vs. $ReRa$ are shown in Fig. 9. Morton's solutions for $Pr = 1$, 0·72 are also shown in the range of small $ReRa$, and the solution is given by

$$\frac{Nu}{Nu_0} = 1 + (0{\cdot}1036 - 0{\cdot}0007\,Pr + 0{\cdot}3334\,Pr^2)\left(\frac{ReRa}{4608}\right)^2 + \ldots$$

where the coefficients of the second term are our collected values, because Morton's results have included some errors.

with the experimental result, because the theoretical curve extended to the range of $ReRa = 10^4$ is not much different from the Morton's curve.

In the present analysis, for the velocity and the temperature distributions in the boundary layer, simple profiles are assumed and particularly in the thin part between the velocity and the thermal boundary layer, the approximation is not good enough. Consequently, equation (57) is correctly applicable to fluids having Prandtl number not far from unity.

In case a large temperature difference exists between fluid and wall, the effect of temperature dependent physical properties should be taken into account with effects of secondary flows.

7. CONCLUSION

Visual experiments and a theoretical analysis for effects of a secondary flow on forced convective laminar heat transfer and flow resistance for a fully developed flow in a horizontal tube

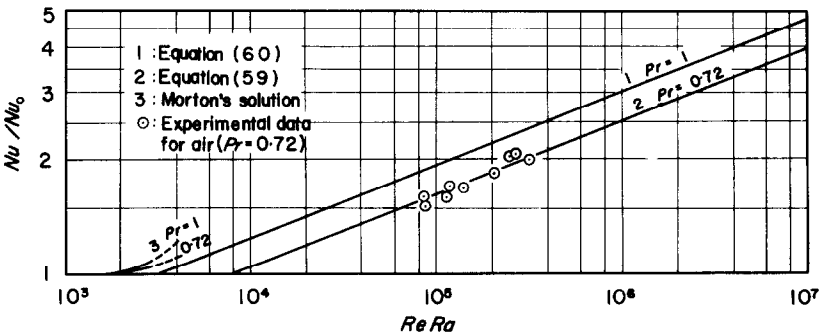

FIG. 9. Nu/Nu_0–$Re\,Ra$ diagram.

The experimental data for air ($Pr = 0{\cdot}72$), expressed in the 1st report are also shown by circles in Fig. 9. For $Pr = 0{\cdot}72$, Nusselt number begins to increase at $ReRa = 10^3$ from Nu_0 (=48/11) with increasing $ReRa$, due to a secondary flow and in very large $ReRa$, it is given by equation (59). As shown in Fig. 9, the theoretical results may be applicable in the range of $ReRa \geqslant 10^4$ and is in good agreement with constant heat flux at the wall have been done and the results obtained are summarized below.

(1) From visual experiments, it is confirmed that the center of the vortex of the secondary flow, due to free convection, comes near to the tube wall with increasing $ReRa$.

(2) On the assumption of a boundary layer

along the tube wall and by use of the boundary-layer integral method, the relations between Nusselt number and $Re\,Ra$ are obtained in the region of Pr not far from unity.

(3) The theoretical results are in comparatively good agreement with the experimental results for air.

(4) Resistance coefficients are given by equation (57) as a function of $Re\,Ra$ and Pr.

REFERENCES

1. B. R. MORTON, Laminar convection in uniformly heated horizontal pipes at low Rayleigh numbers, *Q. Jl Mech. Appl. Math.* **12**, 410–420 (1959).
2. S. T. MCCOMAS and E. R. G. ECKERT, Combined free and forced convection in a horizontal circular tube, *J. Heat Transfer* **88**(2), 147–153 (1966).
3. Y. MORI, K. FUTAGAMI, S. TOKUDA and M. NAKAMURA, Forced convective heat transfer in uniformly heated horizontal tubes, (1st report) Experimental study on the effect of buoyancy, *Int. J. Heat Mass Transfer* **9**(5), 453–463 (1966).
4. M. ADLER, Strömung in gekrümmten Rohren, *Z. Angew. Math. Mech.* **14**, 257–275 (1934).
5. S. N. BARUA, On secondary flow in stationary curved pipes, *Q. Jl Mech. Appl. Math.* **16**, 61–77 (1962).
6. H. ITO, Theoretical and experimental investigation concerning the flow through curved pipes, *Mem. Inst. High Speed Mech., Tohoku Univ.* **14**, 139–172 (1959).
7. Y. MORI and W. NAKAYAMA, Study on forced convective heat transfer in curved pipes, (1st report, laminar region), *Int. J. Heat Mass Transfer*, **8**(1), 67–82 (1965).

Résumé–Les effets de la force d'Archimède sur le transport de chaleur par convection forcée laminaire dans un tube horizontal chauffé uniformement ne peut pas être négligé pour de grandes valeurs de $ReRa$. Ce deuxième rapport at rait à une étude théorique de ce problème dans un écoulement laminaire entièret ment établi et l'on compare ses résultats avec les résultats expérimentaux exposés dans le premier rapport.

Afin de justifier les hypothéses effectuées dans l'analyse qui suit, les configurations d'écoulement secondaire dues à la force d'Archimède sont observées dans des expériences de visualisation d'écoulement. Une solution approchée pour de très grands $ReRa$ est obtenue. Les nombres de Nusselt sont fonctions de $ReRa$ et de Pr, et en assez bon accord avec les résultats expérimentaux sur l'air. Les coefficients de résistance sont aussi obtenus en fonction de $ReRa$ et de Pr.

Zusammenfassung—Der Einfluss der Auftriebskräfte auf den Wärmeübergang bei erzwungener Laminarströmung in einem gleichmässig beheizten waagerechten Rohr darf bei grossen $ReRa$ nicht vernachlässigt werden. Diese zweite Arbeit behandelt eine theoretische Untersuchung des Problems für voll ausgebildete Laminarströmung und vergleicht die Ergebnisse mit den experimentellen Werten der ersten Arbeit.

Um Annahmen der Analyse zu bekräftigen, wurden die Muster der sekundären Auftriebsströmung sichtbar gemacht und beobachtet. Eine Näherungslösung für sehr grosse $Re\,Ra$ liess sich erhalten. Nusselt-Zahlen sind als Funktion von $Re\,Ra$ und Pr wiedergegeben, und es zeigt sich ein ziemlich guter Zusammenhang mit Versuchswerten in Luft. Auch Widerstandskoeffizienten sind als Funktion von $Re\,Ra$ und Pr angegeben.

Аннотация—При больших $Re\,Ra$ нельзя пренебречь влиянием подъемной силы на теплообмен в ламинарном потоке при вынужденной конвекции в однородно нагреваемой горизонтальной трубе. В этой статье дается теоретическое исследование этого вопроса при полностью развитом ламинарном течении, и результаты сравниваются с экспериментальными данными, приведенными в предыдущей статье. Для подтверждения допущений, сделанных в данном анализе, картины вторичного потока за счет подъемной силы наблюдались с помощью визуализации потока. Получено приближенное решение при очень больших $Re\,Ra$. Показано, что числа Нуссельта, выраженные в виде функции $Re\,Ra$ и Pr, хорошо согласуются с экспериментальными результатами для воздуха. Коэффициенты сопротивления также получены в виде функции $Re\,Ra$ и Pr.